Spontaneous symmetry breaking and the dynamics of three interacting nonlinear optical resonators with gain and loss

D. Dolinina* and A. Yulin†
Faculty of Physics, ITMO University, Saint Petersburg 197101, Russia

(Received 8 December 2021; accepted 28 February 2022; published 16 March 2022)

The dynamics of two active nonlinear resonators coupled to a linear resonator is studied theoretically. Possible stationary states and their dynamical stability are considered in detail. Spontaneous symmetry breaking is found and it is shown that this bifurcation results in the formation of asymmetric states. It is also found that the oscillating states can occur in the system in a certain range of parameters. The results of the analysis of the stationary states are confirmed by direct numerical simulations. The possibility of switching between different states is also demonstrated by numerical experiments.

DOI: 10.1103/PhysRevE.105.034203

I. INTRODUCTION

It is well known that a symmetric system always has a symmetric solution. However, this solution must not necessarily be dynamically stable and it can happen that a symmetric system shows a stable asymmetric solution. In some systems, the symmetric solution loses its stability, and switching to an asymmetric state happens when one of the parameters exceeds a threshold value. This is known as spontaneous symmetry breaking (SSB). Such phenomenon is one of the most fundamental processes in nonlinear science, that is why it is under great attention in many fields of physics [1–5] for decades. In particular, SSB appears in many nonlinear optical systems, such as waveguide arrays [6,7], double-well systems [8–10], grated waveguides [11–13], dual-core fibers [14,15], and nonlinear metasurfaces [16,17].

Besides, this effect was found in systems of two- or three-coupled nonlinear waveguides [18–24]. It was shown that the systems of three interacting identical nonlinear couplers [18,19] or of two interacting nonlinear and one linear couplers [20,21,23] provide multistability caused by the appearance of asymmetric states. These systems are especially interesting from the perspective of all-optical device switching. The problem of two nonlinear conservative couplers interacting with a linear conservative coupler is considered in Ref. [21] where different regimes, including chaotic ones, are reported.

In our work we consider a similar system consisting of two nonlinear resonators with linear gain (microlasers) saturated by nonlinear (cubic) losses. We also assume that these active resonators have conservative nonlinearity which makes their resonant frequency dependent on the intensity of the field inside the resonators. The active resonators do not interact with each other directly but both of them are coupled to another resonator situated between them. This resonator is linear with some losses and its resonant frequency is detuned from the resonant frequency of the active resonators in the linear regime. The coupling to this linear resonator introduces the effective coupling between the active resonators. These systems of three resonators we further refer to as trimers. In the present work, we focus on the stationary states and the symmetry breaking that occur in these trimers. We believe that the results reported in the paper are of interest not only from the point of view of applied mathematics but can be used to design switchable multistable sources of coherent light or for all-optical calculations.

Let us remark that the conservative analog of this trimer is considered in Ref. [23] where the symmetry breaking is reported. However, the presence of the dissipative terms affects the bifurcation strongly and, what can be even more important, makes some states to be attractors and thus allows the switching between different stationary states. So the problem of the formation and the switching between the states becomes of interest. For example, below we show that the instability of time-independent states can result in the switching of the trimers to the states where the intensities of the fields in the resonators experience periodic oscillations.

Let us briefly discuss possible physical realizations of such systems. We believe that this can be achieved in the systems of microlasers interacting because of the nonperfect localization of the field inside the resonators. Thus, the resonators separated by small gaps can interact through the evanescent field of their eigenmodes. One of the promising materials for the fabrication of such devices is perovskites that are capable to provide large optical gain and thus obtain lasing in dielectric resonators of small volumes and relatively large radiative losses [25–27].

Another physical realization of the suggested system of the oscillators is exciton-polariton systems where the polariton condensation occurs in the interacting micropillars. These systems are realized experimentally and have been studied for more than a decade [28–33].

It is also worth mentioning that the effect known as bound state in the continuum (BIC) has been actively studied in recent times in optical systems including nonlinear ones

*d.dolinina@metalab.ifmo.ru
†a.v.yulin@corp.ifmo.ru

FIG. 1. The sketch of the considered system.

[34–36]. Indeed, in the case of BIC, the radiation losses disappear because of destructive interference that eliminates the radiation field completely. In the proposed system the coupling to the linear resonator introduces some additional losses for the active nonlinear resonators. The important fact is the effective losses seen by the active resonators depend on the mutual phase of the field in the resonators. Indeed, one can easily see that if the mutual phase is equal to π the total driving force for the middle resonator is equal to zero. So the passive linear oscillator is not excited and, consequently, it does not contribute to the effective losses experienced by the active resonators. This is similar to what happens in BIC systems considered in Ref. [37].

The paper is organized as follows. In the next section we discuss the physical system under consideration and introduce a mathematical model describing the dynamics of the optical fields in the resonators in terms of slow varying amplitudes. In Secs. III–V we do a comprehensive analysis of the antisymmetric, symmetric, and asymmetric stationary states and bifurcations taking place in the active trimers. In Sec. VI we perform a numerical experiment demonstrating the formation of states considered in Secs. III–V. Finally, in the Conclusion, we briefly summarize the main findings reported in the paper.

II. THE PHYSICAL SYSTEM AND ITS MATHEMATICAL MODEL

Let us start with the discussion of the physical system in question. We consider three interacting resonators schematically shown in Fig. 1. Pairs of interacting resonators are often referenced as dimers [22] and, analogously, arrays consisting of three elements are called trimers. In this paper we adopt this terminology [23].

The right and the left resonators have linear gain saturated by nonlinear losses. From the experimental point of view, each of these resonators can be seen as nanolasers pumped above the threshold. These resonators also have Kerr (cubic) nonlinearity so that their resonance frequencies depend on the intensity of the field inside the resonators. Let us note that the Kerr nonlinearity can be called conservative in the sense that it does not change the number of photons whereas the dependency of the photon absorption rate on the intensity of the field we refer to as dissipative nonlinearity.

In this paper, we consider the case when the left and the right resonators are identical. Thus, we consider only symmetric trimers. It is well known that a symmetry of the system does not necessarily mean that the stationary distribution of field in the system must be symmetric, too. For the conservative system the symmetry breaking due to Kerr nonlinearity was considered in Refs. [18,23] and in the present work we study spontaneous symmetry breaking in active optical trimers with relatively strong coupling between the resonators.

To perform the analysis we describe the system by a perturbation method known as the slowly varying amplitude approach, see Refs. [38–40] for details. The method is based on the assumption that the structure of the mode (field distribution) is defined mostly by the shape of the resonator and the refractive indices of the materials of the resonators and the surroundings. The eigenfrequencies and the fields of the resonator eigenmodes can be found solving Maxwell equations for the given geometry and materials. Normally the linear spectrum contains several modes but we restrict our consideration to the case when only one of the modes feels positive linear gain and thus can be excited. We also assume that the difference of the eigenfrequencies of the resonator modes is that big that the interaction (because of Kerr nonlinearity and the other effects) between different modes of the same resonator is negligible.

However, the modes of neighboring resonators can talk to each other provided that the resonators are placed close to each other so that the fields of the modes of the same or close frequencies overlap in space. The interaction strength depends strongly on the overlap of the modes and thus decays rapidly with the distance between the resonators. This allows us to account for the interaction between the nearest neighbors only. So in our trimers, the right and the left resonators having the same parameters do not interact directly but through a middle resonator which is linear and passive and has the eigenfrequency slightly detuned from the frequency of the working modes of the other resonators. All this gives us a possibility to write a set of equations describing the dynamics of the trimers in terms of the slowly varying amplitudes of the left (B), middle (A), and the right (C) resonators:

$$\partial_t B = \Gamma B - \beta|B|^2 B + i\alpha|B|^2 B + i\delta B + i\sigma A, \tag{1a}$$

$$\partial_t C = \Gamma C - \beta|C|^2 C + i\alpha|C|^2 C + i\delta C + i\sigma A, \tag{1b}$$

$$\partial_t A = -\gamma A + i\sigma(B + C), \tag{1c}$$

where γ is the losses in the middle resonator, Γ is linear gain of the left and the right resonators, β characterizes the strength of the nonlinear losses and α is the coefficient of the conservative nonlinearity in active resonators, δ is the detuning of linear resonance frequencies of the left and the right resonators from the frequency of the middle resonator, and σ is the coupling strength of the middle resonator to its neighbors.

Let us acknowledge that the excitation of the linear resonator A depends on the mutual phase of the oscillations in the resonators B and C. One can easily see that there is a mode $B = -C, \quad A = 0$ such that the middle resonator is not excited. It is obvious that there must exist also a mode $B = C, \quad A \neq 0$. It is instructive to rewrite the equations in the form of the "symmetric" $U_s = \frac{B+C}{\sqrt{2}}$ and an "antisymmetric" $U_a = \frac{B-C}{\sqrt{2}}$ modes. In new variables the system of equations for the trimer reads:

$$\partial_t U_s = (\Gamma + i\delta)U_s + (i\alpha - \beta)(K_1 U_s + M U_a) + i\sqrt{2}\sigma A, \tag{2a}$$

$$\partial_t U_a = (\Gamma + i\delta)U_a + (i\alpha - \beta)(K_2 U_a + M^* U_s), \tag{2b}$$

$$\partial_t A = -\gamma A + i\sqrt{2}\sigma U_s. \tag{2c}$$

where $K_1 = \frac{1}{2}(|U_s|^2 + 2|U_a|^2)$, $K_2 = \frac{1}{2}(2|U_s|^2 + |U_a|^2)$ and $M = \frac{1}{2}U_s^* U_a$.

From these equations it is easy to conclude that in the linear regime there are one antisymmetric mode and two symmetric modes with different eigenfrequencies $\omega_a = \delta - i\Gamma$ and $\omega_{s\pm} = \frac{1}{2}[\delta + i(\gamma - \Gamma) \pm i\sqrt{(\gamma + \Gamma + i\delta)^2 - 8\sigma^2}]$ correspondingly. Let us remark, that here and below all frequencies are defined as the detunings from the resonant frequency of the middle resonator (A) of the trimer. It is important for us that the losses of the antisymmetric mode are always lower than the losses of at least one of the symmetric modes. This is the consequence of the symmetry of the system which provides that in the antisymmetric mode the middle resonator is not excited at all.

With the increase of Γ the effective gain of the antisymmetric mode changes its sign and becomes positive. Simple algebra shows that at this Γ the effective gain for both symmetric modes is negative. So the antisymmetric mode exceeds the lasing threshold first. At higher gain Γ the symmetric mode also starts growing. Because of the nonlinearity, the growth of the modes is saturated and a stationary state with constant amplitude can form.

The stationary symmetric and antisymmetric nonlinear solutions can be found in the form $\vec{W}_s = (U_s \neq 0, U_a = 0, A \neq 0)^T$ and $\vec{W}_a = (U_s = 0, U_a \neq 0, A = 0)^T$, respectively. Let us note that these modes have the same symmetry as the linear eigenmodes. However, in the nonlinear regime there may exist the stationary states with all nonzero components $U_s \neq 0$, $U_a \neq 0$, $A \neq 0$. We will refer to these states as hybrid nonlinear states meaning that they can be seen as a sum of symmetric and antisymmetric components. The next sections are devoted to the detailed investigation of the nonlinear states.

III. THE ANTISYMMETRIC STATES OF THE TRIMERS

Now let us consider nonlinear stationary states in more details. The fields in all resonators have the same frequency and thus these states can be sought in a form $A = A_0 e^{i\omega t}$, $B = B_0 e^{i\omega t}$, and $C = C_0 e^{i\omega t}$, where A_0, B_0, and C_0 are unknown complex amplitudes and ω is the frequency of the state, which is also a parameter to be found. The important fact is that Eqs. (1a)–(1c) are invariant in respect to the transformation $\alpha \to -\alpha$, $\delta \to -\delta$, $A \to -A^*$, $B \to B^*$, $C \to C^*$, and $\omega = -\omega$. This means that without loss of generality we can restrict our consideration to either positive or negative sign of Kerr nonlinearity coefficient α. We choose to set α to be positive. Let us also mention that the coupling coefficient σ can also be chosen to be positive without loss of generality because of the invariance of the equations in respect to the transform $\sigma \to -\sigma, A \to -A$.

Let us start with consideration of the antisymmetric states. The nontrivial states of this symmetry exist for $\Gamma > 0$. The amplitude and frequency of antisymmetric states can be found analytically $|B_0| = |C_0| = \sqrt{\Gamma/\beta}$ and $\omega = \alpha\Gamma/\beta + \delta$. We found the areas of existence and analyzed the stability of the state numerically.

To study the stability of the system we can look for a solution in the form $A = [A_0 + a(t)]e^{i\omega t}$, $B = [B_0 + b(t)]e^{i\omega t}$, $C = [C_0 + c(t)]e^{i\omega t}$, where a, b, and c are small perturbations. Substituting this in (1) we obtain the equations for the small perturbations. In these equation we keep only terms that are linear in a, b, and c. To proceed it is convenient to write the equations for the perturbations in vector form introducing $\vec{X} = (\mathrm{Re}(a), \mathrm{Im}(a), \mathrm{Re}(b), \mathrm{Im}(b), \mathrm{Re}(c), \mathrm{Im}(c))^T$,

$$\dot{\vec{X}} = \hat{L}\vec{X},$$

where

$$\hat{L} = \begin{bmatrix} -\gamma & \omega & 0 & -\sigma & 0 & -\sigma \\ -\omega & -\gamma & \sigma & 0 & \sigma & 0 \\ 0 & -\sigma & \Gamma - \beta N(B_0) & \omega - 2\beta M(B_0) & 0 & 0 \\ & & -2\alpha M(B_0) & -\alpha K(B_0) - \delta & & \\ \sigma & 0 & -\omega + \alpha N(B_0) & \Gamma + 2\alpha M(B_0) & 0 & 0 \\ & & +\delta - 2\beta M(B_0) & -\beta K(B_0) & & \\ 0 & -\sigma & 0 & 0 & \Gamma - \beta N(C_0) & \omega - 2\beta M(C_0) \\ & & & & -2\alpha M(C_0) & -\alpha K(C_0) - \delta \\ \sigma & 0 & 0 & 0 & -\omega + \alpha N(C_0) & \Gamma + 2\alpha M(C_0) \\ & & & & +\delta - 2\beta M(C_0) & -\beta K(C_0) \end{bmatrix},$$

is a linear operator governing the dynamics of the small corrections to the resonators amplitudes, where $N(U_0) = 3\mathrm{Re}(U_0)^2 + \mathrm{Im}(U_0)^2$, $M(U_0) = \mathrm{Re}(U_0)\mathrm{Im}(U_0)$, $K(U_0) = \mathrm{Re}(U_0)^2 + 3\mathrm{Im}(U_0)^2$. The solution of this equation is $\vec{X} = \sum_{n=1}^{6} r_n \vec{V}_n \exp(\lambda_n t)$ where λ_n and $\vec{V}_n$ are the eigenvalues and eigenvectors of $\hat{L}$, and r_n are constant defined by the initial perturbation. One can see that if there is at least one λ with positive real part then the perturbation grows exponentially with time and thus the state is unstable. The operator $\hat{L}$ is 6 by 6 matrix and it is easy to find its eigenvalues numerically. Our results of the stability analysis are summarized in Fig. 2 where the instability growth rate of the antisymmetric state is shown as a function of the gain Γ and the detuning δ, the area of the existence of the stable states is shown by black color.

One can see that for sufficiently large positive detunings the state is stable for all values of gain Γ. However, for lower detuning there may exist one or two regions of instability. The bifurcation diagram for the stationary antisymmetric states $\vec{W}_a$ showing the dependence of the field intensity in both laser elements $I = |B|^2 + |C|^2$ on gain Γ is shown in Figs. 3(a) and 3(b) for $\delta = -2.25$ by black color. On the same figure,

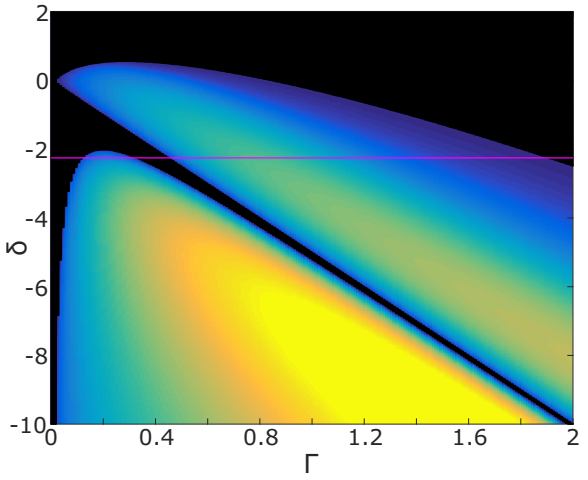

FIG. 2. The growth rate of the unstable perturbations on the parameter plane of the detuning δ and gain Γ for antisymmetric states. Black color corresponds to dynamically stable states ($\max[\mathrm{Re}(\lambda)] \leqslant 0$). The pink line corresponds to the detuning used for the calculation of the bifurcation diagram shown in Fig. 3. Parameters are $\alpha = 0.5$, $\sigma = 1$, and $\beta = 0.1$.

the bifurcation diagrams of the states of the other kinds are shown.

We studied the stability of the antisymmetric state [Fig. 4(a)] and it is found that for negative δ of sufficiently large absolute values both spontaneous symmetry breaking and Andronov-Hopf bifurcations of supercritical and subcritical types take place. First, with the increase of Γ the antisymmetric states become unstable against the perturbations having the structure of the symmetric mode. The motion of the eigenvalues governing the behavior of the weak perturbations of the antisymmetric state is shown in Fig. 4(b). So we can conclude that the symmetry breaking of the antisymmetric state goes through a supercritical pitchfork bifurcation.

As a result of such bifurcation, the hybrid states with nonzero components of both symmetric and antisymmetric modes appear. The bifurcation curve for these states is shown in Fig. 3 by green color. The hybrid states are characterized by nonequal field amplitudes of the resonators $|B| \neq |C|$ and nonzero amplitude of the middle resonator $A \neq 0$, see Fig. 3(c), showing field intensity $|A|^2$ in the middle resonator as a function of the gain. We refer to these asymmetric states as hybrid-I states and will consider them in more detail below.

The analysis shows that at a higher gain the antisymmetric state restores its stability colliding with the hybrid-I states in another pitchfork bifurcation. Let us mention that depending on the detuning this bifurcation can be either super- or subcritical, see Fig. 6.

With the further increase of the gain, the antisymmetric state gets destabilized through a supercritical Hopf bifurcation which gives birth to a periodically oscillating state (a limit cycle in the phase space). The motion of the eigenvalues for this case is shown in Fig. 4(c). Finally, at even higher gain the antisymmetric state restores its stability again through a subcritical Hopf bifurcation, see Fig. 4(a). Let us mention here, that subcritical Hopf bifurcation also results in the appearing of the limit cycle but in this case the limit cycle is unstable.

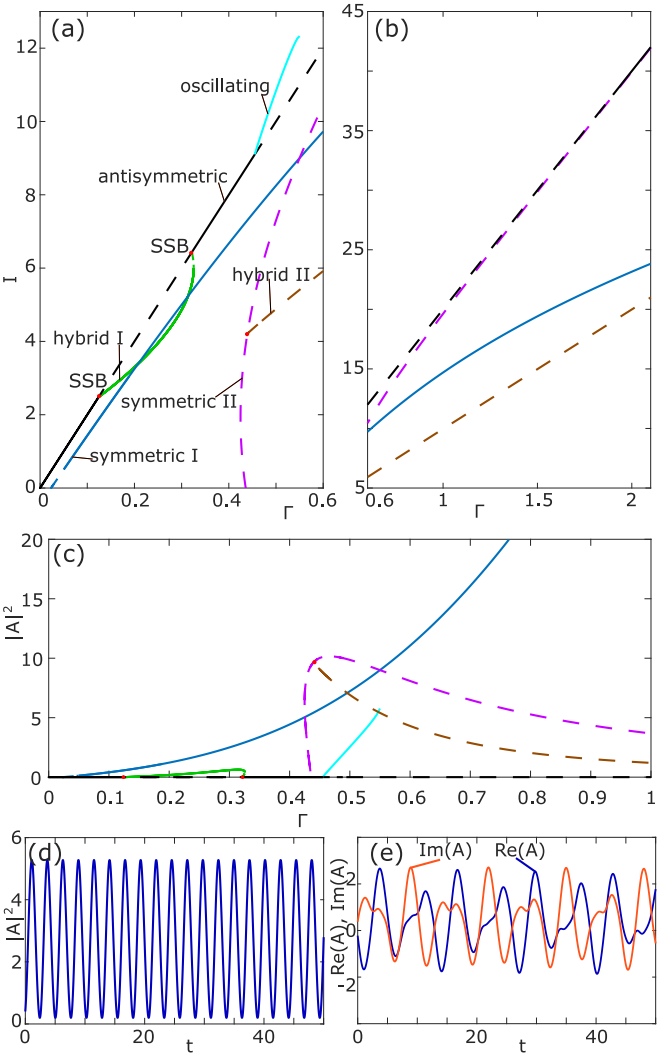

FIG. 3. Bifurcation diagram showing the dependence of field intensity in (a) and (b) active resonators $I = |B|^2 + |C|^2$ and in (c) passive resonator $|A|^2$ of stationary states on the gain Γ. The black line shows the intensity dependence for antisymmetric states; the blue and magenta curves are for the symmetric states; the green and brown lines show the bifurcation curve for the hybrid states. We use dashed lines for the dynamically unstable states and solid lines for the dynamically stable ones. The cyan curves show the maximum amplitude of the periodic state. The red dots mark the spontaneous symmetry bifurcation. Panels (d) and (e) show the dynamics of intensity $|A|^2$ and real/imaginary parts $\mathrm{Re}(A)$, $\mathrm{Im}(A)$ in time of periodic state. Parameters are the same as in Fig. 2, but $\delta = -2.25$.

Let us note that the oscillatory state bifurcating from the antisymmetric one is periodic in terms of absolute values of the fields amplitudes and quasiperiodic in terms of real and imaginary components of amplitudes. To illustrate this we performed numerical simulations and show the temporal dynamics of the intensity of the field and the temporal evolution of the real and imaginary parts of the field in Figs. 3(d) and 3(e). Let us also mention here, that at some threshold linear gain the dynamical state becomes unstable and the instability switches the system into the symmetric state, which will be considered below. The bifurcation curve of the oscillatory

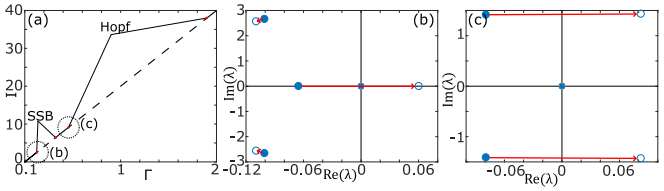

FIG. 4. (a) Bifurcation diagram of the antisymmetric state showing the stability changes of the state. Four eigenvalues with the largest real parts are shown in panel (b) just before (solid circles) and after (open circles) the pitchfork SSB bifurcation. The motion of the eigenvalues for the Hopf bifurcation is shown in panel (c). Red arrows show the motion of eigenvalues during the bifurcation. Zero eigenvalues associated with phase symmetry of (1) are marked by a blue cross in both panels (b) and (c).

state showing the dependence of the maximum intensity of the oscillations on the linear gain Γ is shown in Fig. 3 by the cyan curve within the range of dynamical stability of the state.

The stability of the antisymmetric states becomes different for the detunings $\delta > \delta_{cr1} \approx -2.02$. At $\delta > \delta_{cr1}$ no hybrid states bifurcate from the antisymmetric state. When the detuning exceeds another threshold value $\delta_{cr2} \approx 0.56$ two Hopf bifurcation merge and the antisymmetric state becomes stable for all gain Γ.

IV. HYBRID STATES

Now let us return to the hybrid states. It is worth noting here that the hybrid states appearing as a result of spontaneous symmetry breaking bifurcation are double degenerate. In other words, if $B = B_0$, $C = C_0$, $A = A_0$, and $\omega = \omega_0$ is a solution, then $B = C_0$, $C = B_0$, $A = A_0$ is also a solution having the same frequency ω_0. The area of the existence and the stability of these hybrid-I states are shown in Fig. 5.

First, we consider the bifurcations of the hybrid states for large negative detunings $\delta < -2.26$. As it is said above the hybrid state branching off the antisymmetric state is stable

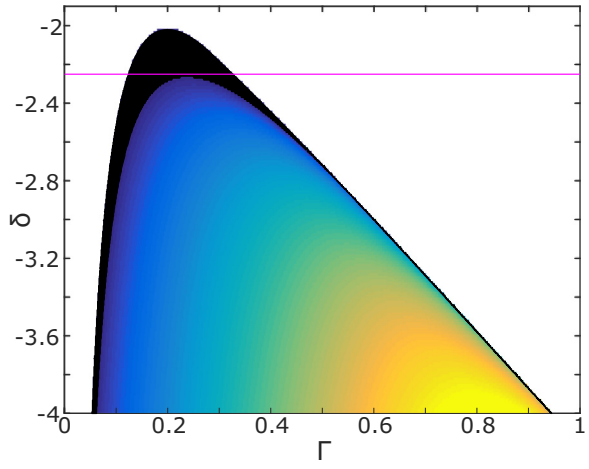

FIG. 5. The growth rate of the unstable perturbations on the parameter plane of the detuning δ and gain Γ for hybrid-I states. The region of parameters where chosen state does not exist is shown by white color.

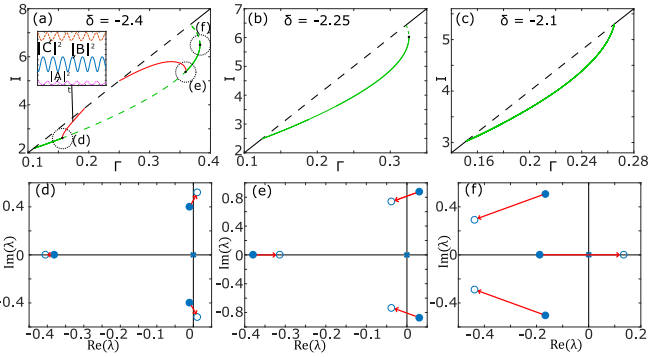

FIG. 6. Panels (a), (b), and (c) show the bifurcation diagrams of the hybrid states for different detunings $\delta = -2.4$, $\delta = -2.25$, and $\delta = -2.1$. Panels (d)–(f) illustrate the motion of the eigenvalues with the largest real parts governing the dynamics of the weak excitations on the hybrid state shown in (a). The solid circles correspond to the eigenvalues before and the open circles to the eigenvalues after the bifurcations. The red arrows show the directions of eigenvalues motions. The red curves in (a) show the maximum amplitudes of dynamically stable limit cycles bifurcated from the hybrid stationary state. The inset in (a) shows temporal dependencies of the field intensities for the case of the oscillating regime.

in the vicinity of the bifurcation point. Then, at a threshold gain, the hybrid state loses its stability via a supercritical Hopf bifurcation, see Figs. 6(a) and 6(d) where the motion of the eigenvalues with the largest real part is shown. As a result of the bifurcation, a stable limit cycle appears. The bifurcation curve for this oscillatory state is shown in Fig. 6(a) by the red line, the dynamics of the field intensities in all three resonators is shown in the inset of Fig. 6(a).

The stability of the hybrid state is restored at a higher gain through another supercritical Hopf bifurcation [the eigenvalues motion is shown in Fig. 6(e)]. Then the hybrid state undergoes fold bifurcation and becomes unstable [the eigenvalues motion is shown in Fig. 6(f)]. Finally, the hybrid states merge with the antisymmetric states via a subcritical pitchfork bifurcation.

With the decrease of the absolute value of the negative detuning Hopf bifurcations of the hybrid-I states collide and disappear at $\delta_{cr3} \approx -2.26$. However, the fold bifurcation of the states survives until $\delta_{cr4} \approx -2.14$. The bifurcation curve of the hybrid state for this case is shown in Fig. 6(b). For higher detunings $\delta > \delta_{cr4}$ the fold bifurcation disappears and the hybrid states merge with the antisymmetric state through a supercritical pitchfork bifurcation, see Fig. 6(c). As one can see, in this case, the hybrid states are stable within the whole range of existence. Finally, the hybrid states cease to exist for $\delta > \delta_{cr1}$.

V. SYMMETRIC STATES

Now let us consider the symmetric states $B = C$, $A \neq 0$. There may be two kinds of these solutions bifurcating from the trivial state. The bifurcation curves for these states are shown in Fig. 3 in blue and magenta colors, correspondingly. The "symmetric-I" state appears at lower gain Γ compared to the "symmetric-II" state and can be seen as a kind of the

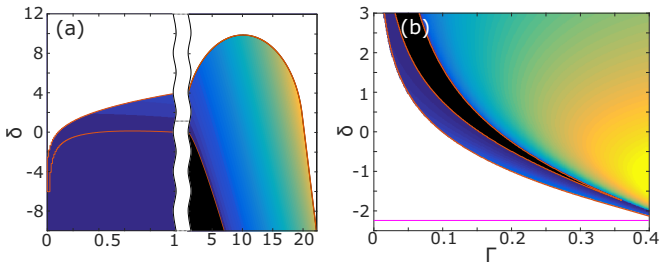

FIG. 7. The growth rate of the unstable perturbations on the parameter plane of the detuning δ and gain Γ for (a) symmetric-I and (b) symmetric-II states.

counterpart of the antisymmetric state. The absolute value of the field in the middle resonator is higher in the "symmetric-I" than in the "symmetric-II" state for the same gain Γ. For the latter state, the ratio of the field intensity in the middle resonator to the field intensity in B (or C) resonator goes to zero with the increase of the gain. This explains why the bifurcation curve of the "symmetric-II" state approaches the bifurcation curve of the antisymmetric state at large Γ, see Fig. 3(b).

The amplitudes of the fields can be found analytically from the system (1) for the symmetric state. To do this we use the fact that for the symmetric states the fields in resonators B and C are the same and then the solution can be sought in the form $B = C = B_0 \exp(i\omega t), A = A_0 \exp(i\omega t)$. Substituting this in (1) we obtain:

$$\omega = \alpha\frac{\Gamma}{\beta} + \delta + \frac{2\sigma^2}{\beta(\gamma^2+\omega^2)}(\beta\omega - \alpha\gamma), \tag{3a}$$

$$|B_0|^2 = \frac{\Gamma}{\beta} - \frac{2\sigma^2\gamma}{\beta(\gamma^2+\omega^2)}, \tag{3b}$$

$$A_0 = 2\sigma\frac{\omega+i\gamma}{\gamma^2+\omega^2}|B_0|. \tag{3c}$$

for the frequency ω and the amplitudes characterizing the state.

The numerical results of the stability analysis for the "symmetric-I" state are summarized in Fig. 7(a). So for $\delta \lesssim \delta_{cr5} \approx -6.1$ "symmetric-I" state is stable until the gain Γ is below a critical value, but the state loses its stability at higher gain through subcritical Hopf bifurcation. Such instability results in the switching of the system to the antisymmetric state. For the intermediate range of detunings $\delta_{cr5} \lesssim \delta \lesssim \delta_{cr6} \approx 0.12$ the "symmetric-I" state becomes unstable at gains close to the excitation threshold, too. This instability is also provided by subcritical Hopf bifurcation; its development leads to the formation of the antisymmetric state. Finally, at δ_{cr6} the stability region of "symmetric-I" state vanishes and then the states are unstable within the whole range of existence $\delta < \delta_{cr7} \approx 9.91$.

The symmetric-II states are also found numerically and it is found that these states can also be stable for $\delta > \delta_{cr8} = -1.8$, the narrow tongue of stability is clearly seen in Fig. 7(b). Decreasing linear gain from the region of stable solutions leads to subcritical Hopf bifurcation and an unstable symmetric state relaxes to the antisymmetric state as a result of the instability development. An increase of the gain leads to spontaneous symmetry breaking bifurcation and appearing of the hybrid states (double degenerated) of the second kind. The bifurcation curve for hybrid-II states is shown in Fig. 3 by the brown dashed curve. Such hybrid states are stable only when bifurcating from the stable symmetric state and have a very narrow stability range. Both symmetric-II and hybrid-II states have small stability areas in the parameter space. On top of it, these stable states have small basins of attractions. Therefore, these states are less interesting from the physical point of view because it seems to be a very hard problem to observe them experimentally.

In the next section we report the results of numerical simulations on the formation of the different nontrivial states from weak noise and the switching between the states.

VI. DIRECT NUMERICAL SIMULATIONS OF THE TRIMER DYNAMICS

The existence of a stable state means that this state can be observed in experiments. However, the basin of attraction of some states is so small that they can form only from the initial conditions very close to the exact stationary solution. It can happen to be difficult to create the necessary initial conditions in the experiment and thus it can be a challenging task to observe these states. Other states can form of the weak noise (random complex values of small amplitude) taken as initial conditions and one can assume that these states are much easier to observe in experiments. In this section we study the formation of the states from the weak noise and the switching of the states caused by the change of the linear gain.

For this purpose, we perform numerical simulation of (1) with Γ varying in time. The procedure of the simulations is as follows. We fix the pump to a constant and perform simulations for the time sufficient for the stationary state to form. In the presented simulations this time is $T = 20\,000$. Then we increase the pump by a small step $\Delta\Gamma = 0.001$ (or $\Delta\Gamma = 0.01$) and continue the simulation obtaining another state. This way we can study how the behavior of the fields changes when the pump is being changed step by step at times $t = N \times 20\,000$, where N is an integer. The simulation is performed with the classical Runge-Kutta method with time step $dt = 0.001$. We set the detuning to be $\delta = -2.4$ because this choice of parameters allows observing the dynamics which is of most interest in the context of the paper.

We start our numerical simulation with the near-zero value of linear gain ($\Gamma = 0.001$) and take the initial conditions in the form of weak noise. As it can be clearly seen from Fig. 8(a) the amplitudes of the fields in both B and C resonators start growing exponentially and the saturation of the growth results in the formation of the antisymmetric state. In the lower part of Fig. 8(a), one can clearly see that the middle resonator A is not excited at all which is a signature of the antisymmetric state. It complies well with the analysis of stationary states summarized in Fig. 3 where one can see that at small values of the gain the antisymmetric state is the only possible stationary solution.

Now we take the antisymmetric solution already formed from the noise and start increasing the gain. When the gain Γ exceeds the threshold of the symmetry breaking bifurcation then the system switches to a hybrid state with broken

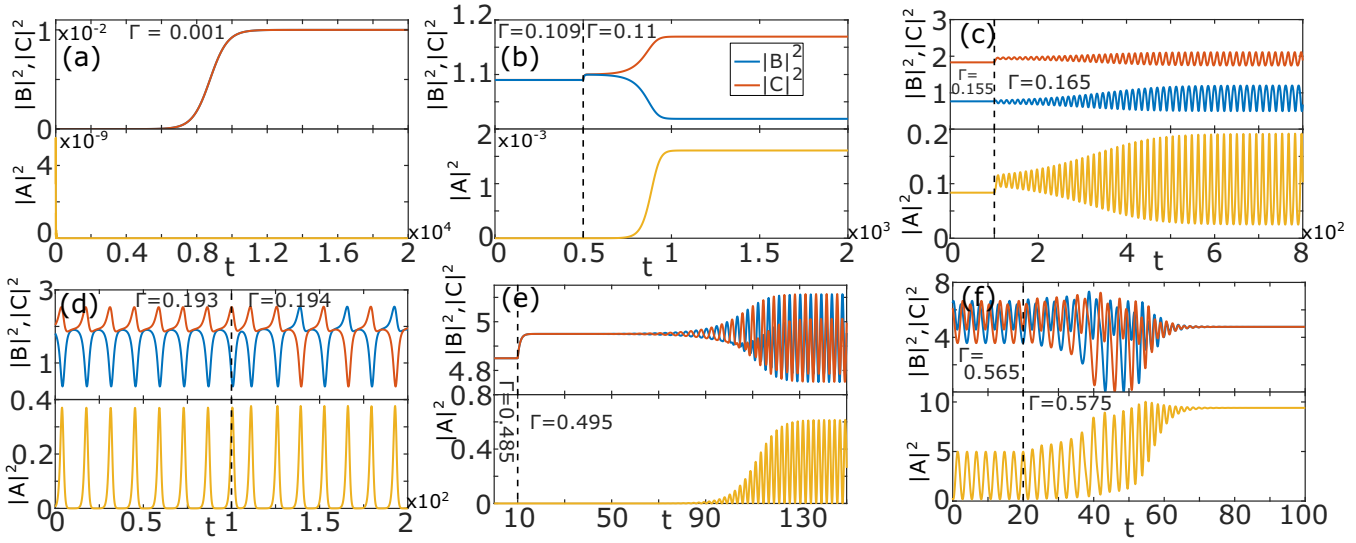

FIG. 8. (a) Evolution in time of the antisymmetric stationary state from the weak initial noise. (b) Switching of the system to the hybrid state by increasing of gain from $\Gamma = 0.109$ to $\Gamma = 0.11$. (c) Appearing of the oscillating state from the hybrid state because of the increase of linear gain to $\Gamma = 0.165$. (d) Switching between two types of oscillating states at $\Gamma = 0.194$. (e) Formation of oscillating state from the antisymmetric state. (f) Switching of the oscillating state into the symmetric state. At each panel beginning of the time interval is shifted to $t = 0$ for convenience of perception. Parameters are the same as in Fig. 2, but $\delta = -2.4$.

symmetry, see Fig. 8(b) showing this switching. One can see that in the final state the intensities of the field in resonator B and C are different and resonator A is excited. An increase of Γ makes the intensity difference between two active resonators larger and the intensity of passive resonator A increases, too.

If the linear gain Γ exceeds the threshold value when the hybrid-I state gets destabilized via supercritical Hopf (see Sec. IV), then the system switches from the hybrid to oscillating state, see Fig. 8(c). Since the oscillating state bifurcates from the stationary state with broken symmetry, the amplitudes of oscillations are different in active resonators. With the increase of Γ the amplitude of the oscillations grows and at some point, the oscillating state switches to another oscillating state, see Fig. 8(d). In the new oscillating state, the amplitudes of the fields in resonators B and C become equal.

It is interesting that by increasing the gain further one can switch the system back to the oscillating state with different amplitudes in resonators B and C and then to a nonoscillating hybrid-I state. It is also observed in numerical simulations that finally the hybrid states restore the symmetry and transform to the antisymmetric state.

Now let us study the destabilization of the antisymmetric states by the Hopf bifurcation. When the linear gain increases the threshold value oscillations of the field intensities start growing destabilizing the system. As a result of this instability a new oscillating state forms, see Fig. 8(e). For this oscillation state, the fields in the resonators B and C oscillate in antiphase. Further increase of the gain leads to destabilization of the oscillating state and the system switches to the symmetric state, see Fig. 8(f). This state is characterized by the high intensity of the field in middle resonator A and is, of course, dynamically stable. We identify the symmetric state as the symmetric-I state described above.

We did not manage to observe hybrid-II and symmetric-II states in numerical simulations that can be explained by small basins of attraction of these states. However, it is important to note that the formation of the antisymmetric, hybrid-I, and symmetric-I states can be easily observed in the system by the appropriate manipulation by the linear gain Γ. At least three different oscillating states can also be observed in the system.

VII. CONCLUSION

In this paper, we have considered the dynamics of the system of two nonlinear active resonators coupled through a linear passive one. The stationary states of such trimer are investigated and classified in terms of symmetry in "antisymmetric," "symmetric," and "hybrid" states. It is demonstrated, that with an antisymmetric state the radiation is locked inside the active resonators because of the destructive interference in the linear one. This state is in a certain sense equivalent to the effect of bound state in the continuum (or BIC) when the radiative losses are completely compensated by the interference effect. The symmetric state, on the contrary, excites the middle resonator which can be seen as an analog of constructive interference increasing the radiative losses in BIC-like systems.

Both antisymmetric and symmetric states are characterized by equal absolute field amplitudes in active resonators. In turn, the hybrid stationary states appear due to a symmetry breaking bifurcation and thus they differ from the symmetric and antisymmetric states having nonidentical field amplitudes in the nonlinear resonators B and C. These hybrid states are characterized by nonzero field in the linear resonator.

The dynamical stability and bifurcations of all the stationary states are analyzed in detail. It is demonstrated, that the state with broken symmetry can bifurcate both from the antisymmetric and the symmetric stationary states. However, the hybrid state bifurcating from the symmetric state has

small basin of attraction, and the region of the pump values where such state is stable is very narrow, thus, to observe the formation of the state one has to prepare the initial state of the system very carefully. This could make the experimental observation of the state to be a challenging problem difficult to solve. The hybrid state bifurcating from the antisymmetric state is stable and the system can be switched to this state starting from random fields of low intensity. At some pump intensities, the state loses its stability through Hopf bifurcation resulting in the formation of the oscillating periodic state.

The formation of the antisymmetric state from weak noise is demonstrated by direct numerical simulations. It is also shown that changing the gain one can transform the antisymmetric states to the hybrid state. By further manipulations with the gain oscillating and the symmetric states can be obtained in the system.

Thus, we can conclude the considered system consisting of three interacting resonators allows us to observe different states and switch them in a controllable way. This can be of interest from the point of view of the design of the dynamically reconfigurable microlasers and find applications in the field of coherent light generation and optical simulations.

ACKNOWLEDGMENTS

This research was supported by Priority 2030 Federal Academic Leadership Program and by the Ministry of Science and Higher Education of Russian Federation, goszadanie no. 2019-1246. Also the authors acknowledge the financial support provided by Russian Fund for Basic Research (Grant "Aspiranty" No. 20-32-90227).

[1] L. Susskind, Dynamics of spontaneous symmetry breaking in the Weinberg-Salam theory, Phys. Rev. D **20**, 2619 (1979).

[2] P. W. Higgs, Broken Symmetries and the Masses of Gauge Bosons, Phys. Rev. Lett. **13**, 508 (1964).

[3] T. Zibold, E. Nicklas, C. Gross, and M. K. Oberthaler, Classical Bifurcation at the Transition from Rabi to Josephson Dynamics, Phys. Rev. Lett. **105**, 204101 (2010).

[4] J. Li, A. K. Harter, J. Liu, L. de Melo, Y. N. Joglekar, and L. Luo, Observation of parity-time symmetry breaking transitions in a dissipative Floquet system of ultracold atoms, Nat. Commun. **10**, 855 (2019).

[5] B. A. Malomed, *Spontaneous Symmetry Breaking, Self-Trapping, and Josephson Oscillations* (Springer, Berlin, 2013).

[6] W. C. K. Mak, Malomed, and P. L. Chu, Asymmetric solitons in coupled second-harmonic-generating waveguides, Phys. Rev. E **57**, 1092 (1998).

[7] R. Driben, B. A. Malomed, and P. L. Chu, All-optical switching in a two-channel waveguide with cubic–quintic nonlinearity, J. Phys. B: At., Mol. Opt. Phys. **39**, 2455 (2006).

[8] M. Matuszewski, B. A. Malomed, and M. Trippenbach, Spontaneous symmetry breaking of solitons trapped in a double-channel potential, Phys. Rev. A **75**, 063621 (2007).

[9] T. Mayteevarunyoo, B. A. Malomed, and G. Dong, Spontaneous symmetry breaking in a nonlinear double-well structure, Phys. Rev. A **78**, 053601 (2008).

[10] G. Chen, Z. Luo, J. Wu, and M. Wu, Switch between the types of the symmetry breaking bifurcation in optically induced photorefractive rotational double-well potential, J. Phys. Soc. Jpn. **82**, 034401 (2013).

[11] S. D. Krasikov, A. A. Bogdanov, and I. V. Iorsh, Nonlinear bound states in the continuum of a one-dimensional photonic crystal slab, Phys. Rev. B **97**, 224309 (2018).

[12] D. Dolinina and A. Yulin, Spontaneous symmetry breaking of nonlinear states in optical cavities with radiative losses, Opt. Lett. **45**, 3781 (2020).

[13] D. Dolinina and A. Yulin, Dissipative switching waves and solitons in the systems with spontaneously broken symmetry, Phys. Rev. E **103**, 052207 (2021).

[14] L. Albuch and B. A. Malomed, Transitions between symmetric and asymmetric solitons in dual-core systems with cubic–quintic nonlinearity, Math. Comput. Simul. **74**, 312 (2007).

[15] Z. Birnbaum and B. A. Malomed, Families of spatial solitons in a two-channel waveguide with the cubic-quintic nonlinearity, Physica D **237**, 3252 (2008).

[16] A. Abrashuly and C. Valagiannopoulos, Photonic memory with nonlinear plasmonic nanotubes, APL Mater. **9**, 101111 (2021).

[17] C. Valagiannopoulos, A. Sarsen, and A. Alù, Angular memory of photonic metasurfaces, IEEE Trans. Antenn. Propag. **69**, 7720 (2021).

[18] C. Schmidt-Hattenberger, R. Muschall, U. Trutschel, and F. Lederer, Nonlinear eigenmodes of a three-core fibre coupler, Opt. Quant. Electron. **24**, 691 (1992).

[19] L. J. Bernstein, The three-waveguide nonlinear directional coupler: The center waveguide excitation, Opt. Commun. **94**, 406 (1992).

[20] M. I. Molina and G. P. Tsironis, Tuning the Kenkre-Campbell self-trapping transition, Phys. Rev. A **46**, 1124 (1992).

[21] M. Molina, W. Deering, and G. Tsironis, Optical switching in three-coupler configurations, Physica D **66**, 135 (1993).

[22] W. Deering, M. Molina, and G. Tsironis, Directional couplers with linear and nonlinear elements, Appl. Phys. Lett. **62**, 2471 (1993).

[23] J. Eilbeck, G. Tsironis, and S. K. Turitsyn, Stationary states in a doubly nonlinear trimer model of optical couplers, Phys. Scr. **52**, 386 (1995).

[24] J. Menezes, W. De Fraga, A. Ferreira, K. Saboia, G. Guimarães, J. Sousa, H. Rocha, A. Sombra *et al.*, Logic gates based in two- and three-modes nonlinear optical fiber couplers, Opt. Quant. Electron. **39**, 1191 (2007).

[25] S. A. Veldhuis, P. P. Boix, N. Yantara, M. Li, T. C. Sum, N. Mathews, and S. G. Mhaisalkar, Perovskite materials for light-emitting diodes and lasers, Adv. Mater. **28**, 6804 (2016).

[26] B. R. Sutherland and E. H. Sargent, Perovskite photonic sources, Nat. Photon. **10**, 295 (2016).

[27] K. Wang, S. Wang, S. Xiao, and Q. Song, Recent advances in perovskite micro-and nanolasers, Adv. Opt. Mater. **6**, 1800278 (2018).

[28] D. Bajoni, P. Senellart, E. Wertz, I. Sagnes, A. Miard, A. Lemaître, and J. Bloch, Polariton Laser using Single Micropillar GaAs−GaAlAs Semiconductor Cavities, Phys. Rev. Lett. **100**, 047401 (2008).

[29] L. Ferrier, E. Wertz, R. Johne, D. D. Solnyshkov, P. Senellart, I. Sagnes, A. Lemaître, G. Malpuech, and J. Bloch, Interactions in Confined Polariton Condensates, Phys. Rev. Lett. **106**, 126401 (2011).

[30] T. Klein, S. Klembt, E. Durupt, C. Kruse, D. Hommel, and M. Richard, Polariton lasing in high-quality selenide-based micropillars in the strong coupling regime, Appl. Phys. Lett. **107**, 071101 (2015).

[31] C. Schneider, K. Winkler, M. D. Fraser, M. Kamp, Y. Yamamoto, E. Ostrovskaya, and S. Höfling, Exciton-polariton trapping and potential landscape engineering, Rep. Prog. Phys. **80**, 016503 (2017).

[32] A. Amo and J. Bloch, Exciton-polaritons in lattices: A nonlinear photonic simulator, C. R. Phys. **17**, 934 (2016).

[33] K. P. Kalinin, A. Amo, J. Bloch, and N. G. Berloff, Polaritonic xy-Ising machine, Nanophotonics **9**, 4127 (2020).

[34] C. W. Hsu, B. Zhen, J. Lee, S.-L. Chua, S. G. Johnson, J. D. Joannopoulos, and M. Soljačić, Observation of trapped light within the radiation continuum, Nature (Lond) **499**, 188 (2013).

[35] C. W. Hsu, B. Zhen, A. D. Stone, J. D. Joannopoulos, and M. Soljačić, Bound states in the continuum, Nat. Rev. Mater. **1**, 16048 (2016).

[36] K. Koshelev, S. Kruk, E. Melik-Gaykazyan, J.-H. Choi, A. Bogdanov, H.-G. Park, and Y. Kivshar, Subwavelength dielectric resonators for nonlinear nanophotonics, Science **367**, 288 (2020).

[37] E. Bulgakov, K. Pichugin, and A. Sadreev, Symmetry breaking for transmission in a photonic waveguide coupled with two off-channel nonlinear defects, Phys. Rev. B **83**, 045109 (2011).

[38] G. P. Agrawal, *Nonlinear Fiber Optics* (Academic Press, San Diego, CA, 2001).

[39] S. Jensen, The nonlinear coherent coupler, IEEE J. Quant. Electron. **18**, 1580 (1982).

[40] A. W. Snyder, Coupled-mode theory for optical fibers, J. Stochast. Anal. **62**, 1267 (1972).